doi:10.1093/brain/awr212 Brain 2011: 134; 2948–2959 | 2948

BRAIN
A JOURNAL OF NEUROLOGY

Data mining neocortical high-frequency oscillations in epilepsy and controls

Justin A. Blanco,[1,2] Matt Stead,[3] Abba Krieger,[4] William Stacey,[5,6] Douglas Maus,[7] Eric Marsh,[8,9] Jonathan Viventi,[2] Kendall H. Lee,[10] Richard Marsh,[10] Brian Litt[2,9] and Gregory A. Worrell[3]

1 Department of Electrical and Computer Engineering, United States Naval Academy, Annapolis, MD, 21402 USA
2 Department of Bioengineering, University of Pennsylvania, Philadelphia, PA, 19104 USA
3 Department of Neurology, Mayo Systems Electrophysiology Laboratory, Mayo Clinic, Rochester, MN, 55905 USA
4 Department of Statistics, The Wharton School, University of Pennsylvania, Philadelphia, PA, 19104 USA
5 Department of Neurology, University of Michigan, Ann Arbor, MI, 48103 USA
6 Department of Biomedical Engineering, University of Michigan, Ann Arbor, MI, 48103 USA
7 Department of Neurology, SUNY Downstate Medical Centre, Brooklyn, NY, 11203 USA
8 Division of Child Neurology, Children's Hospital of Philadelphia, Philadelphia, PA, 19104 USA
9 Department of Neurology, University of Pennsylvania, Philadelphia, PA, 19104 USA
10 Department of Neurosurgery, Mayo Clinic, Rochester, MN, 55905 USA

Correspondence to: J. A. Blanco,
Electrical and Computer Engineering Department,
United States Naval Academy,
Mail Stop 14B, 105 Maryland Avenue,
Annapolis,
MD 21402, USA
E-mail: blanco@usna.edu

Transient high-frequency (100–500 Hz) oscillations of the local field potential have been studied extensively in human mesial temporal lobe. Previous studies report that both ripple (100–250 Hz) and fast ripple (250–500 Hz) oscillations are increased in the seizure-onset zone of patients with mesial temporal lobe epilepsy. Comparatively little is known, however, about their spatial distribution with respect to seizure-onset zone in neocortical epilepsy, or their prevalence in normal brain. We present a quantitative analysis of high-frequency oscillations and their rates of occurrence in a group of nine patients with neocortical epilepsy and two control patients with no history of seizures. Oscillations were automatically detected and classified using an unsupervised approach in a data set of unprecedented volume in epilepsy research, over 12 terabytes of continuous long-term micro- and macro-electrode intracranial recordings, without human preprocessing, enabling selection-bias-free estimates of oscillation rates. There are three main results: (i) a cluster of ripple frequency oscillations with median spectral centroid = 137 Hz is increased in the seizure-onset zone more frequently than a cluster of fast ripple frequency oscillations (median spectral centroid = 305 Hz); (ii) we found no difference in the rates of high frequency oscillations in control neocortex and the non-seizure-onset zone neocortex of patients with epilepsy, despite the possibility of different underlying mechanisms of generation; and (iii) while previous studies have demonstrated that oscillations recorded by parenchyma-penetrating micro-electrodes have higher peak 100–500 Hz frequencies than penetrating macro-electrodes, this was not found for the epipial electrodes used here to record from the neocortical surface. We conclude that the relative rate of ripple frequency oscillations is a potential biomarker for epileptic neocortex, but that larger prospective studies correlating high-frequency oscillations rates with seizure-onset zone, resected tissue and surgical outcome are required to determine the true predictive value.

Keywords: high-frequency oscillations; epilepsy; intracranial EEG

Received December 8, 2010. Revised July 9, 2011. Accepted July 11, 2011

Introduction

Epilepsy affects an estimated 50 million people worldwide (Sander and Shorvon, 1996), with ~30% of patients having seizures that cannot be controlled by medication (Kwan and Brodie, 2000). At present, the best treatment option for this medically refractory population is resective surgery (Lüders and Comair, 2001). Successful surgical treatment of drug-resistant partial epilepsy is based on the concept that the brain areas involved in initiating seizures are well-circumscribed and unchanging, and hence amenable to resection. Technology for localizing epileptogenic regions therefore plays a central role in surgical planning. Intracranial EEG, the recording of electrical activity using electrodes placed directly on or within the brain, is used when non-invasive modalities like scalp EEG, MRI and functional imaging are unable to unambiguously identify the seizure-onset zone. Though some computational methods have been proposed (Bartolomei *et al.*, 2008; Aubert *et al.*, 2009), the clinical gold standard in intracranial EEG-based seizure-onset zone localization remains labour intensive and somewhat subjective visual analysis, whereby neurologists trained to recognize stereotypical epileptiform patterns visually review multi-channel recordings to identify regions that consistently show the earliest departures from non-seizure background activity prior to electrographic seizure onset. Epilepsy surgeries guided by these assessments are often successful in patients with defined MRI abnormalities (Tanriverdi *et al.*, 2008), but outcomes tend to be less favourable for patients who do not have lesions apparent on MRI (Jeha *et al.*, 2007; Bell *et al.*, 2009; Bien *et al.*, 2009).

The search for electrophysiological biomarkers to identify epileptic tissue has motivated the study of transient, quasi-periodic local field potentials within the 100–500 Hz frequency range. These signals, which have durations of tens of milliseconds, are called 'high-frequency oscillations' to distinguish them from the lower frequency activity (0.1–100 Hz) more commonly used in clinical electrophysiology. High-frequency oscillations were initially described in rat hippocampal recordings (O'Keefe, 1976; Buzsaki, 1992) and were later observed in animal parahippocampal (Chrobak and Buzsaki, 1996) and neocortical (Grenier *et al.*, 2001, 2003) structures. The link between high-frequency oscillations and epilepsy was established by the work of Bragin *et al*. (1999), who analysed depth electrode recordings obtained from human subjects with temporal lobe epilepsy. The authors subdivided high-frequency oscillations into two categories, ripples (100–200 Hz) and fast ripples (250–500 Hz), hypothesizing the latter were a pathological marker of epileptogenic brain, while the former were analogous to physiological ripples observed in freely behaving normal rats. More recent studies from human hippocampus (Worrell *et al.*, 2008; Jacobs *et al.*, 2010), however, show that ripple oscillations, as well as fast ripple oscillations, are increased in seizure generating brain regions. In fact, even interictal gamma (30–80 Hz) oscillations are increased in seizure-onset zone in neocortex (Worrell *et al.*, 2004). These studies demonstrating an increase in activity previously defined as physiological, i.e. gamma and ripple frequency oscillations, highlight the difficulty in epileptic brain of attaching pathological specificity to high-frequency oscillation subclasses based on oscillation frequency (Traub, 2003; Engel *et al.*, 2009).

The pathological specificity of a particular high-frequency oscillation is further complicated by the fact that high-frequency oscillations of the same frequency may have different mechanisms of generation. Ripple oscillations in the hippocampal CA1 region of freely behaving normal rats reflect summed inhibitory postsynaptic potentials resulting from synchronous interneuron input (Ylinen *et al.*, 1995), but also can be generated by bursts of pyramidal cell population spikes (Bragin *et al.*, 2007). Physiological ripple oscillations are thought to be important in declarative memory consolidation (Wilson and McNaughton, 1994), but oscillations in the same frequency range have also been implicated in seizure generation, as mentioned above, and epileptogenesis (Bragin *et al.*, 2004). The mechanism(s) underlying the generation of fast ripples are less clear (Dzhala and Staley, 2004; Foffani *et al.*, 2007). Fast ripples are more frequently associated exclusively with pathology in the literature, but, as discussed above, the notion that ripples are normal and fast ripples are epileptic is probably overly simplistic (Traub, 2003; Engel *et al.*, 2009).

Whether the relationship of high-frequency oscillations to seizure-onset zone is the same in neocortex as it is in hippocampus, given the phylogenetic and structural differences between the two regions, also remains unclear. In addition, systematic characterization of high-frequency oscillations in normal human brain for baseline comparison has not been possible in any brain region because of the invasiveness of intracranial recordings. The ability to obtain electrophysiological recordings from normal controls was critical in demonstrating the association of high-frequency oscillations with epileptic areas in kainic acid-treated rats (Bragin *et al.*, 2004). There has been a pressing need for similar control data for human high-frequency oscillation research, which has until now been limited to epileptic brain.

A final factor complicating the study of high-frequency oscillations in epilepsy has been selection bias arising from the need to reduce data volume for manual review. In prior work (Blanco *et al.*, 2010), our group demonstrated an algorithm for automated detection and classification of high-frequency oscillations that eliminates the need for manual intervention and does not assume the existence of any specific high-frequency oscillation subclasses, i.e. ripples and fast ripples. Here, we quantitatively analyse the outputs of that algorithm in a group of nine patients with neocortical epilepsy and two control patients with no history of seizures. We address three open questions about the relationship between neocortical high-frequency oscillations and seizure generation and the electrodes required to record them: (i) Are high frequency oscillations rates (events/second) different in control patients and non-seizure-onset zone in patients with epilepsy?; (ii) are high-frequency oscillation rates different within and outside the seizure-onset zone (in patients with epilepsy)?; and (iii) do micro-electrodes record high-frequency oscillations of higher frequency than macro-electrodes, as might be expected if fast ripples are spatially more localized than ripples?

Materials and methods

Data and subject description

The data set we analyse is comprised of 219 756 putative high-frequency oscillations recorded from the neocortices of 11 human subjects undergoing evaluation at Mayo Clinic with subdural electrode arrays. Nine subjects with medically refractory partial epilepsy believed to be of neocortical origin had electrodes implanted as part of routine clinical care. The location, number and type (e.g. grid and/or strip) of intracranial electrodes were determined by a multi-disciplinary team including neurosurgeons, neurologists, neuroradiologists and neuropsychologists. Standard clinical grid and strip electrodes were modified under an Institutional Review Board approved research protocol by adding arrays of non-penetrating platinum–iridium micro-wires (40 μm diameter, with intra-array spacing of 0.5–1 mm centre-to-centre) between the clinical, 4-mm diameter contacts (Van Gompel *et al.*, 2008; Worrell *et al.*, 2008). Two 'control' patients with intractable face pain but no history of seizures were similarly implanted, as part of an unrelated Institutional Review Board-approved research protocol investigating electrical stimulation of motor cortex as a potential treatment for their condition. Table 1 summarizes the clinical characteristics and electrode placements for each subject.

Depth electrodes were also implanted in some subjects. Standard clinical depth leads were modified in two ways: (i) by embedding micro-wires around the circumference of the lead-body between the 2.3-mm long clinical contacts; and (ii) by passing a bundle of micro-wires within the lumen of the lead, so that they protruded by ~7–8 mm from the distal tip (Worrell *et al.*, 2008). To ensure that our conclusions pertain to neocortex, depth electrode data are excluded from all but one analysis (Fig. 4B), whose purpose is precisely to contrast epipial neocortical surface electrode with intra-parenchymal depth electrode results. Insufficient amounts of depth electrode data precluded comparative analyses elsewhere. Informed consent was obtained after the nature and possible consequences of the studies were explained to subjects.

Signal acquisition and processing

Continuous, long-term data were acquired using the Digital Lynx Data Acquisition System (Neuralynx, Inc.) at 32 556 samples per second and 20 bits per sample (stored), from up to 144 channels in each patient (Brinkmann *et al.*, 2009). The input dynamic range was ±132 mV and the noise level was ~1.3 μV root mean square, yielding ~18 effective bits. Recordings were made using direct current capable amplifiers, and a 9 kHz analogue low-pass filter was employed to minimize aliasing effects. The bandwidth of the raw recordings was thus approximately 0–9 kHz.

Event data were extracted from the raw intracranial EEG using a three-stage process detailed in Blanco *et al.* (2010). Briefly, in the first stage, which was originally tested and applied in patients with epilepsy (Staba *et al.*, 2002), candidate events were detected within non-overlapping 10 min windows of 100–500 Hz bandpass filtered intracranial EEG (after decimation by a factor of 12, to 2713 Hz), on a per channel basis. Amplitude and duration thresholds were applied to the short-time energy of the signal in each window; flagged segments were then subject to waveform shape criteria to ensure robust oscillatory characteristics (Csicsvari *et al.*, 1999*a*, *b*; Staba *et al.*, 2002; Gardner *et al.*, 2007). In the second stage, a Gaussian mixture model of the local background intracranial EEG (~2.5 s) surrounding each candidate was learned using the Expectation Maximization Algorithm (Dempster *et al.*, 1977), and events bearing too large a spectral similarity to background according to the model were discarded from candidacy. In the final stage, events were clustered using the *k*-medoids algorithm (Hastie *et al.*, 2001), with the gap statistic (Tibshirani *et al.*, 2001) used to determine the optimal number of clusters. The approach yielded four clusters that we analyse here.

Localization of seizure-onset zone

For each patient, all recorded seizures were visually identified and independently reviewed by two board-certified epileptologists prior to data analysis. The time of the earliest intracranial EEG change was noted and the associated macro-electrode(s) were selected as the electrographic seizure-onset zone. Time of earliest intracranial EEG change was determined by identifying a clear electrographic seizure discharge in a macro-electrode recording and then looking backward in the record for the earliest change from background contiguously associated with the discharge. As micro-electrode recordings were not used in clinical determination of the seizure-onset zone, their labels were extrapolated from those of the macro-electrodes; a micro-electrode was given the label of seizure-onset zone if it belonged to a cluster immediately adjacent to a non-peripheral seizure-onset zone macro-electrode.

Because regions outside the seizure-onset zone displaying prominent interictal epileptiform activity are often considered for surgical resection along with seizure-onset zone, we also defined the 'irritative zone' and 'non-irritative zone' for analysis (Lüders and Comair, 2001). An electrode (macro or micro) was considered an irritative zone electrode if it was either (i) a seizure-onset zone electrode; or (ii) an electrode immediately adjacent to a seizure-onset zone electrode and displaying prominent interictal spiking activity.

Statistical analyses

Control versus non-seizure-onset zone groups

A permutation test was used to test the null hypothesis that there was no difference in the average median event rate between control and non-seizure-onset zone groups. The permutation distribution was generated by taking all 55 (11-choose-2) possible groups of 9 (the number of subjects with epilepsy) and 2 (the number of control subjects) and computing the difference between the average median event rates for the two groups. Separate tests were carried out for each of the four clusters, and for macro- and micro-electrodes, yielding eight total tests.

Seizure-onset zone versus non-seizure-onset zone channels

Because of the large variability in median event rates across subjects with epilepsy, and because not all subjects were represented in all channel classes—for example, only two subjects had surface micro-electrodes in the physician-labelled seizure-onset zone—we chose not to aggregate across subjects in studying the difference between seizure-onset zone and non-seizure-onset zone channels. For each patient for whom the comparison was possible, using event rate as the measured variable on channels, we tested the null hypothesis that the cumulative distribution function for seizure-onset zone channels was equal to that for non-seizure-onset zone channels. (This same test is also commonly, if less accurately, described as a test for a difference between the medians of two groups.) Separate analyses were carried out for each of the four clusters, and for macro- and micro-electrodes, yielding a maximal total of eight tests per patient. The Mann–Whitney U-test was used to test the null hypotheses, with the Bonferroni adjustment made to account for multiple comparisons. We also

Table 1 Patient and implanted electrode characteristics

Subject	Age	Gender	Epilepsy risk factor	Pre-op MRI	Surgery	Path	Outcome	Electrode types	Electrode placements
CT01	44	F	n/a	Normal	n/a	n/a	n/a	4 × 4 hybrid	Right motor
CT02	46	F	n/a	Normal	n/a	n/a	n/a	4 × 6 hybrid	Left motor
SZ01	35	F	Oligodendroglioma. Previous resection	Encephalomalacia	Right frontal corticectomy	Oligodendroglioma and gliosis	ILAE-1, f/u = 22 months	6 × 6 standard, 1 × 8 hybrid	Right frontal, motor
SZ02	24	M	None	Focal region of increased T_2 signal in left frontal lobe	Left frontal corticectomy	Cortical dysplasia (Taylor type I)	ILAE-2, f/u = 32 months	4 × 6 hybrid, 6 × 6 standard	Left frontal, left frontoparietal
SZ03	21	F	Traumatic braininjury, left frontal head at age 1	Increased T_2 signaland left HC atrophy; left frontal encephalomalacia	Left anterior temporal lobectomy	Severe subpial gliosis	ILAE-5, f/u = 19 months	1 × 4 standard, 1 × 4 standard, 1 × 4 hybrid, 1 × 8 standard, 1 × 4 hybrid, 1 × 4 hybrid, 1 × 4 standard depth, 1 × 4 standard depth	Anterior left subfrontal, middle left subfrontal, posterior left subfrontal, anterior left mesial temporal, middle left subtemporal, posterior left subtemporal, anterior, posterior
SZ04	39	F	None	Normal	Left anterior temporal lobectomy	Marked gliosis, predominantly subcortical and subpial; temporal lobe	ILAE-1, f/u = 39 months	6 × 6 standard, 1 × 8 standard, 1 × 8 standard, 1 × 4 standard, 1 × 4 standard, 1 × 4 hybrid depth, 1 × 4 standard depth	Left temporal, left inferior frontal, left superior frontal, left temporal anterior, left temporal posterior, left anterior, left posterior
SZ05	21	F	None	Normal	Left temporal corticectomy	Subpial gliosis	ILAE-1, f/u = 28 months	4 × 6 standard, 1 × 4 standard, 1 × 4 standard, 1 × 4 standard, 1 × 8 standard, 1 × 4 hybrid, 1 × 4 standard, 1 × 4 standard	Left temporal, anterior temporal, anterior mesial temporal, mesial temporal, posterior temporal, frontal, anterior depth, middle depth, posterior depth
SZ06	42	M	Ependymoma, resected at the age of 10 years	Encephalomalacia	Left parietal corticectomy	Marked subpial gliosis; recurrence of ependymoma	Single post-op seizure, f/u = 36 months	4 × 6 hybrid, 6 × 8 standard	Left parietooccipital, left frontoparietal
SZ07	42	F	None	Abnormal T_2 signal, right frontotemporal white matter; lesion, frontal horn of right lateral ventrical	Right frontal corticectomy	Dyslpasia and gliosis	ILAE-1, f/u = 4 months	6 × 8 standard, 3 × 8 standard, 1 × 4 hybrid, 1 × 4 standard, 1 × 8 hybrid	Right frontal, right temporal, right anterior temporal, right inferior temporal, right posterior temporal
SZ08	38	F	Closed head injury	normal	Left anterior temporal lobectomy	Severe subpial gliosis	ILAE-1, f/u = 25 months	6 × 6 standard, 1 × 4 hybrid depth, 1 × 4 hybrid depth, 1 × 4 standard depth	Left temporal, left anterior temporal, middle temporal, posterior temporal
SZ09	27	M	Astrocytoma, resected at the age of 10 years	Encephalomalacia	Right frontal corticectomy	Encephalomalacia; previous astrocytoma resection	ILAE-2, f/u = 20 months	8 × 8 standard, 1 × 4 standard, 1 × 4 hybrid, 1 × 8 standard, 1 × 4 hybrid, 1 × 4 standard, 1 × 4 standard	Right frontal, superior right interhemispheric, inferior right interhemispheric, right frontopolar, superior right lateral temporal, inferior right lateral temporal

f/u = follow-up; ILAE = International league against epilepsy; n/a = not applicable.

performed the above-mentioned seizure-onset zone/non-seizure-onset zone analyses using irritative zone/non-irritative zone instead. Additionally, we carried out both the latter and former analyses using only those high-frequency oscillations that were identified during non-seizure epochs. Non-seizure epochs were defined as those falling outside of a board-certified epileptologist's markings of seizure onset and offset, plus 10 min on either side of these delimiters.

Macro- versus micro-electrodes

For each of the 219 756 neocortical surface events, we computed the frequency within the 100–500 Hz frequency band having maximal power ('peak frequency') using a multi-taper method from Thomson (1982) [three tapers; 512-point Discrete Fourier Transform (zero-padded); adaptive nonlinear combination method). We tested the null hypothesis that the cumulative distribution functions of event peak 100–500 Hz frequencies were equal for macro- and micro-electrodes, with the alternative hypothesis being that the micro-electrode distribution was stochastically larger. The Mann–Whitney U-test was used for the comparison. The same was then done for the 70 517 depth electrode events.

Results

High-frequency oscillation characteristics

Across 11 subjects, a total of 219 756 putative high-frequency oscillations (100–500 Hz) were automatically detected on neocortical surface channels and clustered by the algorithm detailed in Blanco *et al.* (2010) and reviewed above. Four unique clusters were discovered and their relation to variables of clinical interest was analysed.

Twenty-nine per cent (63 652) of all high-frequency oscillation detections belonged to a cluster (Cluster 2) determined to be consistent with artefact, characterized by sharp, non-physiological voltage transients in the raw data. The sharpness of these large amplitude transients yielded high frequency ringing when bandpass filtered, thereby generating false positive detections (Blanco *et al.*, 2010). Of the remaining putatively physiological events, 41% (64 392) belonged to a cluster (Cluster 1) characterized by mixed frequency, irregular waveforms; 11% (16 691) belonged to a cluster (Cluster 3) characterized by relatively fast, regular waveforms; and 48% (75 021) belonged to a cluster (Cluster 4) characterized by relatively slow, regular waveforms. Figure 1 shows five randomly selected examples from each of the four clusters, illustrating these properties.

Table 2 provides descriptive statistics for each cluster—the medians and interquartile ranges of four quantities: (i) the ratio of the integrated power spectral density estimate in the 250–500 Hz frequency band to that in the 100–200 Hz band (power ratio); (ii) the centroid of the power spectral density within the 100–500 Hz frequency band (spectral centroid); (iii) the line length of the spectrally equalized time-domain signal (Usui and Amidror, 1982; Gardner *et al.*, 2007), normalized by signal duration (line length); and (iv) the peak of the power spectral density in the

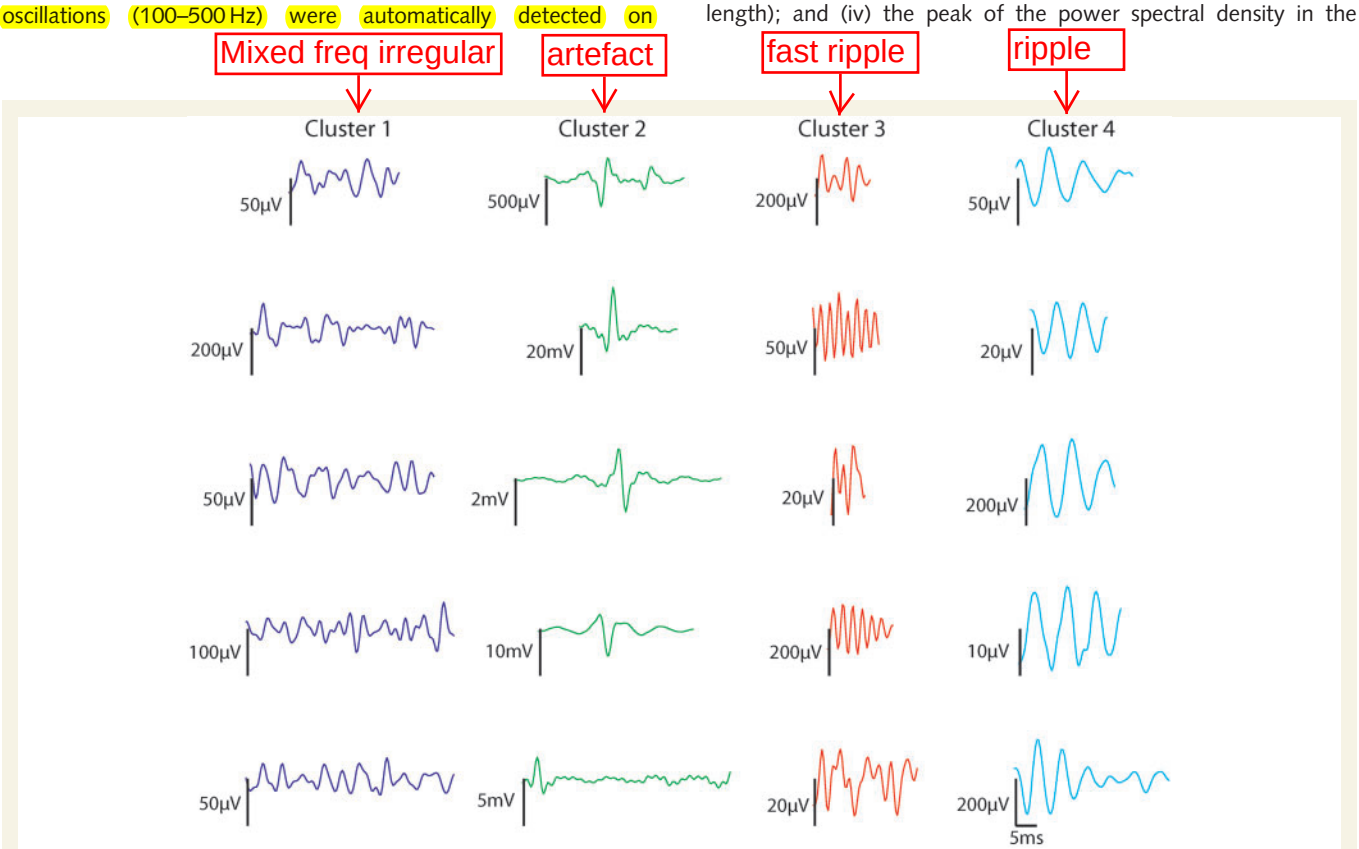

Figure 1 Cluster member examples. Five randomly selected waveforms from each of the four clusters found using the automated detection and unsupervised classification method of Blanco *et al.* (2010). Waveforms are 100–500 Hz bandpass filtered segments corresponding to detections (truncated to 25 ms, if necessary, to put all waveforms on the same time scale for comparison).

100–500 Hz band (spectral peak). Since these quantities represent a subset of the features used to derive the clusters themselves [additional features used in clustering were global/average-local peak ratio; entropy of the squared and normalized Teager energy vector; and a wavelet packet-based energy feature (Blanco *et al.*, 2010)], statistical comparison of their values across groups (using, for example, non-parametric analysis of variance methods) is not appropriate. Nonetheless, examining the values in Table 2 gives a sense for the between-group differences that drove the clustering.

It can be seen, for example, that Cluster 3 events tend to have higher peak 100–500 Hz frequencies than Cluster 4 events. Furthermore, the relative proximity of the spectral centroid value to the spectral peak value in Clusters 3 and 4, compared with Clusters 1 and 2, suggests that the former pair have their power concentrated in a narrower band within 100–500 Hz than the latter—supporting the description 'regular waveforms' for Clusters 3 and 4 in the discussion above. Clusters 1 and 2 appear primarily distinguished by their line length values, which is consistent with the observation that Cluster 2 events are characterized by sharp transients; that is, large sample-to-sample voltage differences that would contribute to high line-length values are present for a relatively smaller fraction of the overall segment duration in Cluster 2 versus Cluster 1 events. Cluster 1 events have spectral centroid values that are intermediate between those of Clusters 3 and 4, supporting the observation that Cluster 1 events tend to have relatively strong spectral components in both the 100–200 Hz and 250–500 Hz bands, and leading to their qualitative description as 'irregular waveforms.' Cluster 3 events have a median peak frequency that is consistent with what prior studies have identified as 'fast ripples', and Cluster 4 events with what have been identified as 'ripples.'

Channel statistics by patient

Table 3 shows event rates for the aggregate of Clusters 1 ('mixed'), 3 ('fast ripple') and 4 ('ripple') (i.e. all but the 'artefact' cluster), broken down by patient and by channel class. Each cell in columns 2–5 gives the median aggregate event rate and the interquartile range; the corresponding number of channels is shown in the last column, and column 6 gives the total number of channel hours of data recorded per patient. The table provides important context for the statistical analyses of the following sections, making sample sizes clear and indicating where data are unavailable. For seven of the eight subjects—all but SZ02—with epilepsy for whom the comparison can be made, the median macroelectrode aggregate event rate is higher in the seizure-onset zone than the non-seizure-onset zone; the same is true for

Table 2 Cluster statistics

Feature	Cluster 1 (n = 64 392)	Cluster 2 (n = 63 652)	Cluster 3 (n = 16 691)	Cluster 4 (n = 75 021)
Power ratio	0.82 (0.99)	0.83 (1.02)	3.73 (3.20)	0.04 (0.11)
Spectral centroid (Hz)	219 (49)	220 (50)	305 (37)	137 (35)
Line length (AU)	0.031 (0.012)	0.007 (0.009)	0.024 (0.030)	0.026 (0.011)
Spectral peak (Hz)	193 (61)	167 (64)	302 (87)	146 (32)

Entries are median (interquartile range).
AU = arbitrary units.

Table 3 Channel statistics

Subject	Non-seizure-onset zone ($x10^{-4}$ events/s)		Seizure-onset zone ($x10^{-4}$ events/s)		CH (h)	NC (counts)
	Macro	Micro	Macro	Micro		
CT 01	26.9 (17.7)	14.3 (19.7)	–	–	1176	16,128,0,0
CT 02	13.5 (8.7)	8.7 (11.3)	–	–	1877	24,104,0,0
SZ 01	2.3 (3.1)	11.7 (8.1)	49.0 (131.3)	–	480	34,6,5,0
SZ 02	13.4 (14.1)	10.2 (11.2)	12.8 (0.0)	12.6 (8.6)	1890	22,79,1,24
SZ 03	31.4 (12.3)	37.8 (29.6)	32.6 (0.0)	–	864	27,33,1,0
SZ 04	18.5 (7.9)	9.4 (8.5)	18.9 (4.7) -	–	1921	51,28,3,0
SZ 05	19.3 (7.9)	–	22.9 (4.3)	–	2860	33,0,11,0
SZ 06	2.7 (2.7)	8.0 (8.3)	7.8 (1.7)	8.4 (7.3)	10139	17,25,6,67
SZ 07	24.0 (16.8)	0.0 (8.3)	35.2 (14.1)	–	5615	57,22,7,0
SZ 08	5.1 (1.5)	–	–	–	234	36,0,0,0
SZ 09	2.0 (1.2)	0.0 (1.6)	2.9 (0.7)	–	735	81,22,7,0

Entries are median event rate (interquartile range), where an 'event' is any member of Clusters 1, 3 or 4 (i.e. putative artefact Cluster 2 excluded).
CH = channel hours: the sum over all channels of the length of time recorded for each channel; NC = number of channels: (macro-non-seizure-onset zone zone, micro-non-seizure-onset zone, macro-seizure-onset zone, micro-seizure-onset zone).

micro-electrodes for the two subjects for whom the comparison can be made. In seven of the nine patients with epilepsy, micro-electrode recordings were not available from both seizure-onset zone and non-seizure-onset zone. Figure 2 complements Table 3, showing the average proportion of events falling into each of the four clusters, broken down by patient and channel class. Clusters are coloured in accordance with Fig. 1. Two main trends are apparent in subjects whose pie charts represent more than a single channel (SZ02 and SZ03 each have only one macro-electrode in the seizure-onset zone): (i) Cluster 3 (red, 'fast ripple') typically accounts for the smallest proportion of events; and (ii) Cluster 4 (cyan, 'ripple') typically accounts for a greater proportion of events in seizure-onset zone compared with non-seizure-onset zone channels. Below, we test whether the trends towards higher event rates in the seizure-onset zone, apparent in Table 3 and Fig. 2, are statistically significant, disaggregating clusters in order to discern which are responsible for any significant effects.

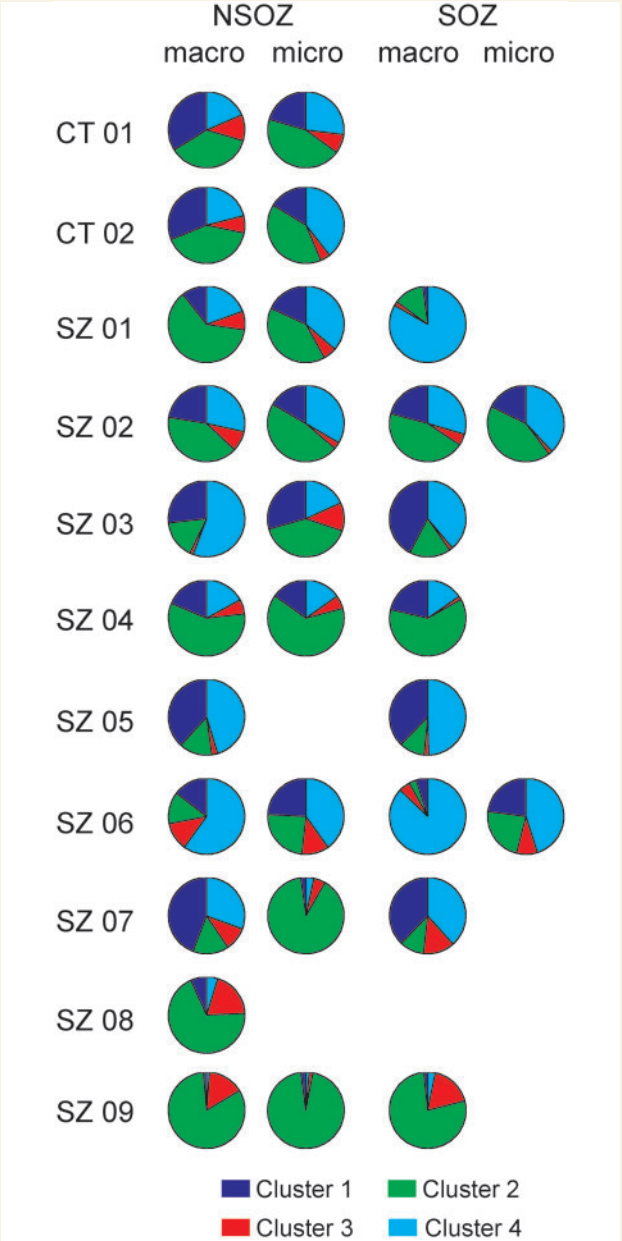

Figure 2 Subject-channel events by cluster. The area of each pie chart wedge corresponds to the mean proportion of events in a given cluster. Blue = Cluster 1 ('mixed frequency'); green = Cluster 2 (putative artefact); red = Cluster 3 ('fast ripple'); and cyan = Cluster 4 ('ripple'), where the mean is over all channels in the category defined by the row and column of the pie. Empty cells in the table indicate that no data were available. CT01 and CT02 are the control patients; SZ01–SZ09 are the subjects with epilepsy. Macro = macro-electrode; micro = micro-electrode; NSOZ = non-seizure-onset zone; SOZ = seizure-onset zone.

can we then treat non soz/irritative zone hfo recordings as baseline

Control versus non-seizure-onset zone groups

Even at the liberal α level of 0.1, no significant differences in high-frequency oscillation rates were found between non-seizure-onset zone in patients with epilepsy and controls. For both micro- and macro-electrodes, the average median event rates for Clusters 1 ('mixed'), 2 ('artefact'), 3 ('fast ripple') and 4 ('ripple'), respectively, obtained from control versus non-seizure-onset zone were not significantly different based on the permutation tests. The small number of control subjects limits the statistical power, but there is no evidence to reject the null hypothesis of no difference in event rates between control and the non-seizure-onset zone of patients with epilepsy. We also compared control and seizure-onset zone high-frequency oscillation rates, separately for micro- and macro-electrodes, finding no significant differences for any of the four high-frequency oscillation clusters [though, notably, for macro-electrodes the *P*-value for Cluster 4 ('ripples') was substantially lower than those for the other three clusters].

WOW!!!

Seizure-onset zone versus non-seizure-onset zone channels

We compared event rates on seizure-onset zone channels to non-seizure-onset zone channels on an individual subject basis, by electrode type (macro or micro) and by cluster. For micro-electrodes, no significant differences were found between seizure-onset zone and non-seizure-onset zone for any of the clusters, in either of the patients for whom the comparison could be made. For macro-electrodes, no significant differences between seizure-onset zone and non-seizure-onset zone were found in any of the patients for Clusters 1 ('mixed'), 2 ('artefact') or 3 ('fast ripple'). These results remained unchanged when we included the irritative zone in the analysis, i.e. replacing the seizure-onset zone/non-seizure-onset zone comparison with the irritative zone/non-irritative zone comparison.

For Cluster 4 ('ripple'), five of the eight subjects (63%) for whom the comparison could be made showed an increasing trend in high-frequency oscillation rates on seizure-onset zone macro-electrodes compared with non-seizure-onset zone. In four of these subjects, the median event rates on seizure-onset zone macro-electrodes was marginally or significantly higher than for non-seizure-onset zone. Uncorrected *P*-values for the Mann–Whitney U-test for these subjects—SZ01, SZ05, SZ06 and

SZ07—were 0.00036, 0.037, 0.00069 and 0.098, respectively. The marginally significant (at $\alpha = 0.1$) results for Patients SZ05 and SZ07 do not survive the Bonferroni correction. For the irritative zone/non-irritative zone comparison, however, the results for SZ07 do remain significant after Bonferroni correction (with all other results remaining unchanged).

The box plots of Fig. 3 summarize the results of the non-seizure-onset zone to seizure-onset zone comparisons for macro-electrodes in these four subjects. The right side of each panel in Fig. 3 shows Cluster 4 ('ripple') high-frequency oscillation rates for individual channels in a given patient, with the bars corresponding to seizure-onset zone channels coloured in red. A trend towards high Cluster 4 ('ripple') high-frequency oscillation rates on seizure-onset zone channels is evident in each plot. Particularly for Subjects SZ06 and SZ07, however, not all channels with relatively high Cluster 4 ('ripple') high-frequency oscillation rates were marked by clinicians as being in the seizure-onset zone.

Notably, none of the results described in this section were materially changed when we analysed only those high-frequency oscillations occurring in non-seizure epochs.

Macro- versus micro-electrodes

In contrast to the findings from human temporal lobe (Worrell *et al.*, 2008), in neocortex, we found no evidence ($P \approx 1$) to reject the null hypothesis of no difference in favour of the alternative hypothesis that the distribution of event peak 100–500 Hz frequencies is stochastically larger for micro-electrodes than macro-electrodes. As can be seen in Fig. 4A, the distributions for macro-electrode events ($n = 130\,098$) and micro-electrode events ($n = 89\,658$) look qualitatively similar, and the medians are close (macro-median, interquartile range: 170 Hz, 69 Hz; micro-median, interquartile range: 164 Hz, 61 Hz). In fact, a *post hoc* two-sided Mann–Whitney U-test finds evidence for the opposite effect ($P << 0.001$), namely that macro-electrodes have a tendency to record events with peak 100–500 Hz frequencies that are slightly higher than those for micro-electrodes. The low *P*-value for such an apparently small effect is not surprising given the large sample sizes.

Figure 4B, on the other hand, shows a result that does agree with findings from temporal lobe. It depicts the same two distributions as in Fig. 4A, but for depth electrodes, which were implanted in four of the nine seizure patients (SZ03, SZ04, SZ05 and SZ08) in addition to surface electrodes. Depth macro-electrodes yielded 11 179 events on 40 total channels in these four subjects. Depth micro-electrodes, only present in two of the four subjects, yielded 59 338 events on 84 total channels. In Fig. 4B, the distributions show a strong qualitative difference. The medians are much farther apart than for the surface electrodes (macro-median, interquartile range: 167 Hz, 58 Hz; micro-median, interquartile range: 209 Hz, 154 Hz). Here, the one-sided Mann–Whitney U-test, with alternative hypothesis that micro-electrodes have larger peak (100–500 Hz) event frequencies than macro-electrodes, leads us to strongly reject the null hypothesis of no difference ($P << 0.0001$).

Discussion

The main findings reported are: (i) in a group of neocortical patients with epilepsy, using automated detection and classification techniques without any manual data pre-selection, we found a class of high-frequency oscillations corresponding to ripple frequency oscillations whose rate of occurrence is increased in the physician-labelled seizure-onset zone in 63% of the patients and marginally or significantly increased in 50%; (ii) a class of oscillations corresponding to fast ripple high-frequency oscillations is relatively rare, and does not show significant rate increases in the neocortical seizure-onset zone compared with non-seizure-onset zone; (iii) we found no evidence that control neocortex is different from neocortex outside the seizure-onset zone in patients with epilepsy, when considering the rate at which high-frequency oscillations (of perhaps different underlying mechanisms) are generated; and (iv) while micro-electrodes on the neocortical surface do not appear to preferentially record high-frequency oscillations of higher frequency, micro-electrodes embedded in the parenchyma do.

Spontaneous 100–500 Hz high-frequency oscillations have been rarely studied systematically in human epileptic neocortex, and high-frequency oscillation statistics from control neocortex of patients without a history of seizures are reported here for the first time, to our knowledge. We analysed more than 200 000 automatically detected high-frequency oscillation candidates in neocortical recordings from nine epilepsy and two control patients, originating in over 27 000 channel hours of intracranial EEG. Though our number of subjects was comparable with prior studies of high-frequency oscillations in human epilepsy, the overall volume of data we processed (>12 terabytes) was significantly larger. We hypothesize that analysing multi-hour continuous recordings permits more reliable estimates of global high-frequency oscillation rates across brain states than, for example, the short (e.g. 10 min) intracranial EEG segments typically examined under the constraints of human processing. Larger data sets also tend to produce more stable statistical estimates of the number of high-frequency oscillation classes (Blanco *et al.*, 2010).

The finding of an increase in neocortical ripple frequency high-frequency oscillations in the seizure-onset zone is consistent with prior studies that used human-intensive processing (Worrell *et al.*, 2008; Jacobs *et al.*, 2009). That there were two particular subjects whose seizure-onset zone increases were detected despite several non-seizure-onset zone channels with comparable ripple-like rates raises the possibility that some seizure-generating areas were missed by the clinical seizure mapping process, which currently does not take high-frequency oscillations into account. The finding that fast ripple-like events are rare and not significantly increased in the neocortical seizure-onset zone is different than previous studies investigating mesial temporal lobe epilepsy (Bragin *et al.*, 1999; Worrell *et al.*, 2008), but in reasonable accord with one study that reported that >200 Hz high-frequency oscillations were not observed in the four subjects with neocortical epilepsy that they studied (Crépon *et al.*, 2010). Urrestarazu *et al.* (2007) also report fast ripples only rarely in neocortex. They reported fast ripple seizure-onset zone rate increases in a

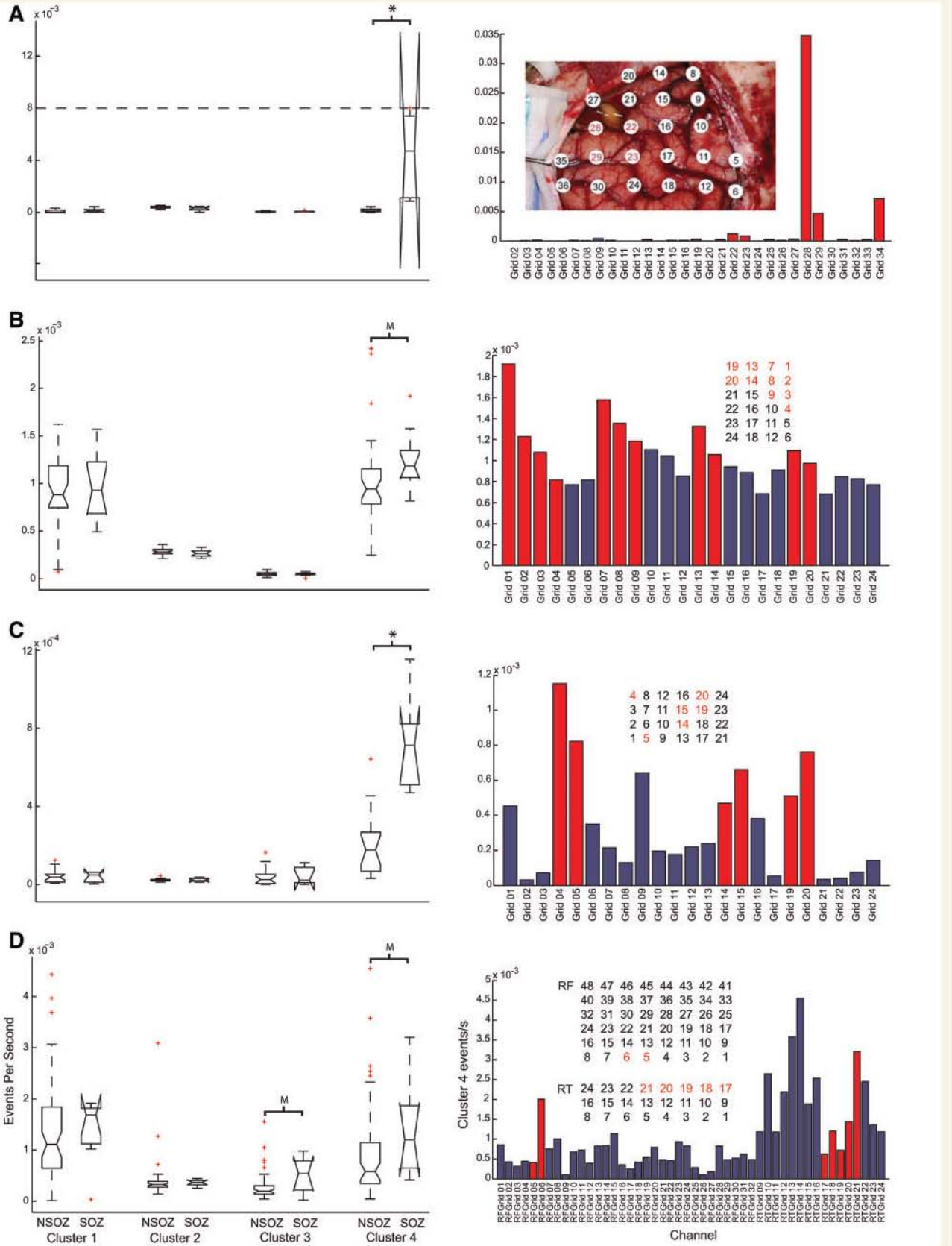

Figure 3 Non-seizure-onset zone versus seizure-onset zone. Macro-electrode data for subject SZ01 (**A**), SZ05 (**B**), SZ06 (**C**) and SZ07 (**D**). On the left side in each panel, there are two box-and-whisker plots for each of the four detected high-frequency oscillation clusters, one corresponding to non-seizure-onset zone channels (*left*) and one to seizure-onset zone channels. On each box, the central mark is the median event rate (counts/s) and the edges are the 25th and 75th percentiles. Whiskers extend to the most extreme data points not

(continued)

small number of patients, but the rate increases did not reach statistical significance. The absence of an increase in fast ripple high-frequency oscillations in neocortex reported here could be related to the fact that our epipial micro-wires are unlikely to detect neuronal unit activity. However, this seems unlikely to be the complete explanation as multiple groups have reported the ability to record fast ripple high-frequency oscillations from clinical macro-electrodes, which would not capture single unit or multi-unit neuronal activity.

The three subjects without increasing trends in Cluster 4 ('ripple') seizure-onset zone rates all had fewer than three macro-electrodes in the seizure-onset zone, including two subjects with only a single macro-electrode in the seizure-onset zone. A fourth subject, SZ09, anomalously had median rates of zero on both seizure-onset zone and non-seizure-onset zone channels; and though the median rate was thus not higher in seizure-onset zone channels for this subject, the mean rate was higher, by a factor of 1.7. High percentages of non-seizure-onset zone and seizure-onset zone channels without any Cluster 4 ('ripple') events was not surprising for this subject, given the uniquely poor quality of Subject SZ09's recordings, which is evidenced by the predominance of the colour green (Cluster 2, putative artefact) in the plots in Fig. 2. The average number of seizure-onset zone electrodes was 4-fold higher in the five subjects with increasing Cluster 4 ('ripple') trends in the seizure-onset zone. We suspect that the number of subjects in whom statistical significance was retained after correction for multiple comparisons would have been larger had the number of seizure-onset zone electrodes been greater. Unfortunately, this sampling limitation, discussed in greater detail below, is inevitable given the spatial density of current clinical electrode arrays. We anticipate that new high-density electrode array technology will be able to resolve this limitation in future work (Kim *et al.*, 2010; Viventi *et al.*, 2010).

We observed events of all four classes in both control patients. Moreover, event rates for control regions were not significantly different for any cluster when compared with non-seizure-onset zone regions. With only two control patients, our permutation tests had relatively low power. But they are discouraging for the prospect of finding a universally 'normal' rate of high-frequency oscillations that might serve as a baseline for patient-independent detection of the seizure-onset zone.

does the electrode size affect recording of fast ripples?

We are uncertain how to interpret the finding that micro-electrodes record high-frequency oscillations of higher frequency than macro-electrodes on depth but not surface electrodes. Given the cellular architectural differences between hippocampus, for example, and neocortex, it is plausible that this result reflects physiological differences in the micro-environments of depth and surface electrodes. An alternative explanation might be related to the fact that surface micro-electrodes are non-penetrating and rest atop the pia mater, which may act as a low-pass filter, while the depth micro-electrodes actually penetrate the parenchyma.

Our data-mining approach (as well as subsequent analyses) treats all intracranial EEG equally. On one hand, this can be viewed as a limitation: our methods do not explicitly attempt to parse whether high-frequency oscillation detections are occurring during specific states of arousal, or in conjunction with epileptiform events such as sharp waves, or within or outside of lesions, for example. That said, other authors have investigated these questions, concluding that the spatial specificity of high-frequency oscillations may be improved in non-REM sleep (Bagshaw *et al.*, 2009) and that high-frequency oscillations provide localizing information independent from interictal spikes (Jacobs *et al.*, 2008), lesions (Jacobs *et al.*, 2009) and seizures themselves (Worrell *et al.*, 2008).

On the other hand, this unbiased algorithmic approach leads to several ideas about high-frequency oscillations in epilepsy. First, the fact that we found a signal that increases in the seizure-onset zone without special selection of patients, channels or time-epochs for processing, suggests that the signal is strong. Second, it suggests that similar findings in prior studies of high-frequency oscillations in mesial temporal lobe, which typically use restrictive data pre-selection criteria, may actually be more generalizable, and hence potentially more practically useful in the clinical setting. Finally, that we are able to detect and classify these signals automatically, without any human intervention, adds to the promise of practical clinical utility. The results presented here support the usefulness of unbiased automated detection of high-frequency oscillations from large data sets, and the potential application to pre-surgical evaluations. The results also open a potential therapeutic opportunity with the possibility that high-frequency oscillations can be used as control signals in closed loop-implantable seizure therapy devices, which will not have the same luxury of human expert review to pre-identify optimal data for processing.

Figure 3 Continued
considered outliers, defined as points >1.5 times the interquartile range above the 75th percentile or below the 25th percentile and plotted individually as red crosses. Dotted line in top left panel represents an arbitrary value to which a single large outlier (34.7×10^{-3}) was clipped for visualization purposes. Notch widths are computed according to McGill *et al.* (1978); lack of notch overlap is a rough test for significant differences in medians at the 5% significance level; we use the Mann–Whitney U-test on the distributions to more formally test significance. On the right side in each panel, Cluster 4 event rates are shown for the individual channels of all electrodes containing seizure-onset zone contacts. Where channel numbers are not continuous, data were not available. Bars corresponding to seizure-onset zone channels are coloured in red, and the spatial arrangement of channels is given in the inset maps, in which seizure-onset zone channels are also coloured red. The map for (**A**) was superimposed on a brain image using the method of Wellmer *et al.* (2002). Channels located beneath the dura are not depicted, but their locations are readily inferred. Space constraints prohibited including comparable images for the other subjects; these can be found in Supplementary Fig. 1. NSOZ = non-seizure-onset zone; SOZ = seizure-onset zone. Asterisks indicate Bonferroni corrected *P*-value for Mann–Whitney U-test < 0.1; M = marginally significant at α level 0.1, but does not survive the Bonferroni correction.

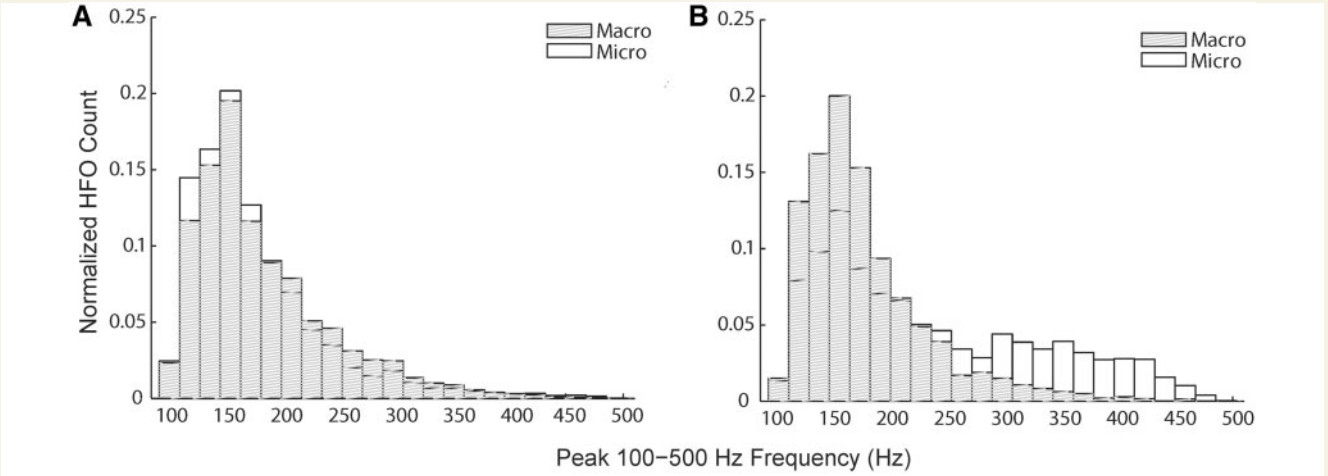

Figure 4 Event peak frequency. Histogram density estimates for the peak 100–500 Hz frequency of events (Clusters 1–4, aggregated) on micro- (white) and macro- (hatched) electrodes, for surface (**A**) and depth (**B**) electrodes. HFO = high-frequency oscillation.

Our findings should be interpreted in light of limitations on electrode coverage. By nature, clinical intracranial EEG recordings suffer from significant spatial undersampling (Stead *et al.*, 2010). Electrode implants span a limited range of cortex surrounding the suspected seizure-onset zone, often leaving doubt as to whether important seizure-generating regions have been missed. For a study like ours, this means both noise in the labels of seizure-onset zone and non-seizure-onset zone, particularly where electrodes near the periphery of an array are concerned; and less than optimal sample sizes (i.e. numbers of channels in a given group), often making it difficult to detect all but very large effects statistically. Another potential sampling limitation in this study is that intraparenchymal cortical recordings were not performed. It is possible that some classes of high-frequency oscillations, such as the fast ripples found in penetrating micro-electrode recordings in the hippocampus, are most reliably recorded from penetrating neocortex as well.

The efficacy of epilepsy surgery and implantable anti-epileptic devices is directly linked to precise identification of seizure-generating regions. Our results suggest that automated mapping of high-frequency oscillations may be of significant utility for this purpose, though it is important to underscore that the finding of a statistically significant relationship between seizure-onset zone regions and high-frequency oscillation increases does not necessarily imply good surgical outcome predictive value. It is still an open question, for instance, whether high-frequency oscillation activity on a given channel can be used to make reliable predictions about whether the tissue beneath that channel should be resected to improve the chances of favourable surgical outcome. Our findings remain to be associated with outcome and should be validated in larger prospective studies.

As clinical results for patients undergoing surgery for non-lesional neocortical epilepsy have plateaued at only modest rates, we hope that a better understanding of the spatial and temporal characteristics of high-frequency oscillations in epileptic networks will lead to improved surgical outcome.

Acknowledgements

We thank Ed Nieh, Cindy Nelson, Karla Crockett and Stacey Seidl for assistance with data management and Steve Isard for valuable technical discussions.

Funding

National Institute of Neurological Disorders and Stroke (R01 NS-041811 and R01 NS-48598 to B.L., R01 NS-630391 to G.A.W., and U24 63930 to B.L. and G.A.W); the Epilepsy Foundation (grant to J.A.B.); the Robert S. Morison fellowship through the Grass Foundation and American Epilepsy Society (grant to D.M.); the Dr Michel and Mrs Anna Mirowski Discovery Fund for Epilepsy Research (grant to B.L.); the National Institutes of Health (K08 NS-52232 to K.H.L.); and the Mayo Foundation Research Early Career Development Award for Clinician Scientists (grant to K.H.L.).

Supplementary material

Supplementary material is available at *Brain* online.

References

Aubert S, Wendling F, Regis J, McGonigal A, Figarella-Branger D, Peragut J-C, et al. Local and remote epileptogenicity in focal cortical dysplasias and neurodevelopmental tumours. Brain 2009; 132: 3072–86.

Bagshaw AP, Jacobs J, LeVan P, Dubeau F, Gotman J. Effect of sleep stage on interictal high-frequency oscillations recorded from depth macroelectrodes in patients with focal epilepsy. Epilepsia 2009; 50: 617–28.

Bartolomei F, Chauvel P, Wendling F. Epileptogenicity of brain structures in human temporal lobe epilepsy: a quantified study from intracerebral EEG. Brain 2008; 131 (Pt 7): 1818–30.

Bell ML, Rao S, So ES, Trenerry M, Kazemi N, Stead SM, et al. Epilepsy surgery outcomes in temporal lobe epilepsy with a normal MRI. Epilepsia 2009; 50: 2053–60.

Bien CG, Szinay M, Wagner J, Clusmann H, Becker AJ, Urbach H. Characteristics and surgical outcomes of patients with refractory magnetic resonance imaging–negative epilepsies. Arch Neurol 2009; 66: 1491–9.

Blanco JA, Stead M, Krieger A, Viventi J, Marsh WR, Lee KH, et al. Unsupervised classification of high-frequency oscillations in human neocortical epilepsy and control patients. J Neurophysiol 2010; 104: 2900–12.

Bragin A, Engel J Jr, Wilson CL, Fried I, Buzsaki G. High-frequency oscillations in human brain. Hippocampus 1999; 9: 137–42.

Bragin A, Wilson CL, Almajano J, Mody I, Engel J Jr. High-frequency oscillations after status epilepticus: epileptogenesis and seizure genesis. Epilepsia 2004; 45: 1017–23.

Bragin A, Wilson CL, Engel J Jr. Voltage depth profiles of high-frequency oscillations after kainic acid-induced status epilepticus. Epilepsia 2007; 48 (Suppl. 5): 35–40.

Brinkmann BH, Bower MR, Stengel KA, Worrell GA, Stead M. Large-scale electrophysiology: acquisition, compression, encryption, and storage of big data. J Neurosci Methods 2009; 180: 185–92.

Buzsaki G. High-frequency network oscillation in the hippocampus. Science 1992; 256: 1025–7.

Chrobak JJ, Buzsaki G. High-frequency oscillations in the output networks of the hippocampal-entorhinal axis of the freely behaving rat. J Neurosci 1996; 16: 3056–66.

Crépon B, Navarro V, Hasboun D, Clemenceau S, Martinerie J, Baulac M, et al. Mapping interictal oscillations greater than 200 Hz recorded with intracranial macroelectrodes in human epilepsy. Brain 2010; 133: 33–45.

Csicsvari J, Hirase H, Czurko A, Mamiya A, Buzsaki G. Fast network oscillations in the hippocampal CA1 region of the freely behaving rat. J Neurosci 1999a; 19: RC20.

Csicsvari J, Hirase H, Czurko A, Mamiya A, Buzsaki G. Oscillatory coupling of hippocampal pyramidal cells and interneurons in the behaving rat. J Neurosci 1999b; 19: 274–87.

Dempster AP, Laird NM, Rubin DB. Maximum likelihood from incomplete data via the EM algorithm. J Roy Stat Soc Series B Methodol 1977; 39: 1–38.

Dzhala VI, Staley KJ. Mechanisms of fast ripples in the hippocampus. J Neurosci 2004; 24: 8896–906.

Engel J Jr, Bragin A, Staba R, Mody I. High-frequency oscillations: what is normal and what is not? Epilepsia 2009; 50: 598–604.

Foffani G, Uzcategui YG, Gal B, Menendez de la Prida L. Reduced spike-timing reliability correlates with the emergence of fast ripples in the rat epileptic hippocampus. Neuron 2007; 55: 930–41.

Gardner AB, Worrell GA, Marsh E, Dlugos D, Litt B. Human and automated detection of high-frequency oscillations in clinical intracranial EEG recordings. Clin Neurophysiol 2007; 118: 1134–43.

Grenier F, Timofeev I, Steriade M. Focal synchronization of ripples (80-200 Hz) in neocortex and their neuronal correlates. J Neurophysiol 2001; 86: 1884–98.

Grenier F, Timofeev I, Steriade M. Neocortical very fast oscillations (Ripples, 80-200 Hz) during seizures: intracellular correlates. J Neurophysiol 2003; 89: 841–52.

Hastie T, Tibshirani R, Friedman J. The elements of statistical learning. New York: Springer; 2001.

Jacobs J, LeVan P, Chander R, Hall J, Dubeau F, Gotman J. Interictal high-frequency oscillations (80-500 Hz) are an indicator of seizure onset areas independent of spikes in the human epileptic brain. Epilepsia 2008; 49: 1893–907.

Jacobs J, LeVan P, Chatillon C-E, Olivier A, Dubeau F, Gotman J. High frequency oscillations in intracranial EEGs mark epileptogenicity rather than lesion type. Brain 2009; 132: 1022–37.

Jacobs J, Zijlmans M, Zelmann R, Chatillon C-E, Hall J, Olivier A, et al. High-frequency electroencephalographic oscillations correlate with outcome of epilepsy surgery. Ann Neurol 2010; 67: 209–20.

Jeha LE, Najm I, Bingaman W, Dinner D, Widdess-Walsh P, Lüders H. Surgical outcome and prognostic factors of frontal lobe epilepsy surgery. Brain 2007; 130: 574–84.

Kim D, Viventi J, Amsden J, Xiao J, Vigeland L, Kim Y, et al. Dissolvable films of silk fibroin for ultrathin conformal bio-integrated electronics. Nat Mat 2010; 9: 511–7.

Kwan P, Brodie M. Early identification of refractory epilepsy. New Engl J Med 2000; 342: 314–9.

Lüders HO, Comair YG. Epilepsy surgery. 2nd edn. Philadelphia, PA: Lippincott Williams and Wilkins; 2001.

McGill R, Tukey JW, Larsen WA. Variations of box plots. Am Stat 1978; 31: 12–6.

O'Keefe J. Place units in the hippocampus of the freely moving rat. Exp Neurol 1976; 51: 78–109.

Sander J, Shorvon S. Epidemiology of the epilepsies. J Neurol, Neurosurg, Psychiatry 1996; 61: 433–43.

Staba RJ, Wilson CL, Bragin A, Fried I, Engel J Jr. Quantitative analysis of high-frequency oscillations (80–500 Hz) recorded in human epileptic hippocampus and entorhinal cortex. J Neurophysiol 2002; 88: 1743–52.

Stead M, Bower M, Brinkmann BH, Lee K, Marsh WR, Meyer FB, et al. Microseizures and the spatiotemporal scales of human partial epilepsy. Brain 2010; 133: 2789–97.

Tanriverdi T, Olivier A, Poulin N, Andermann F, Dubeau F. Long-term seizure outcome after mesial temporal lobe epilepsy surgery: corticalamygdalohippocampectormy versus selective amygdalohippocampectomy. J Neurosurg 2008; 108: 517–24.

Thomson DJ. Spectrum estimation and harmonic analysis. Proc IEEE 1982; 9: 1055–96.

Tibshirani R, Walther G, Hastie T. Estimating the number of clusters in a data set via the gap statistic. J Roy Stat Soc Series B 2001; 63: 411–23.

Traub RD. Fast oscillations and epilepsy. Epilepsy Curr 2003; 3: 77–9.

Urrestarazu E, Rahul C, Dubeau F, Gotman J. Interictal high-frequency oscillations (100-500 Hz) in the intracerebral EEG of epileptic patients. Brain 2007; 130: 2354–66.

Usui S, Amidror I. Digital low-pass differentiation for biological signal processing. IEEE Trans Biomed Eng 1982; BME-29: 686–93.

Van Gompel JJ, Stead SM, Giannini C, Meyer FB, Marsh WR, Fountain T, et al. Phase I Trial: safety and feasibility of intracranial electroencephalography using hybrid subdural electrodes containing macro- and microelectrode arrays. Neurosurg Focus 2008; 25: 1–6.

Viventi J, Kim D, Moss J, Kim Y, Blanco JA, Annetta N, et al. A conformal, bio-interfaced class of silicon electronics for mapping cardiac electrophysiology. Sci Transl Med 2010; 2: 24ra2.

Wellmer J, von Oertzen J, Schaller C, Urbach H, Konig R, Widman G, et al. Digital photography and 3D MRI-based multimodal imaging for individualized planning of resective necortical epilepsy surgery. Epilepsia 2002; 43: 1543–50.

Wilson MA, McNaughton BL. Reactivation of hippocampal ensemble memories during sleep. Science 1994; 265: 676–9.

Worrell G, Parish L, Cranstoun SD, Jonas R, Baltuch G, Litt B. High-frequency oscillations and seizure generation in neocortical epilepsy. Brain 2004; 127: 1496–506.

Worrell GA, Gardner AB, Stead SM, Hu S, Goerss S, Cascino GJ, et al. High-frequency oscillations in human temporal lobe: simultaneous microwire and clinical macroelectrode recording. Brain 2008; 131: 928–37.

Ylinen A, Bragin A, Nadasdy Z, Jando G, Szabo I, Sik A, et al. Sharp wave-associated high-frequency oscillation (200 Hz) in the intact hippocampus: network and intracellular mechanisms. J Neurosci 1995; 15: 30–46.